Journal of Medicinal Chemistry
Brief Article

J. Med. Chem. **2011,** *54,* 1101–1105 **1101**
DOI: 10.1021/jm101181u

3-Thiomorpholin-8-oxo-8*H*-acenaphtho[1,2-*b*]pyrrole-9-carbonitrile (S1) Based Molecules as Potent, Dual Inhibitors of B-Cell Lymphoma 2 (Bcl-2) and Myeloid Cell Leukemia Sequence 1 (Mcl-1): Structure-Based Design and Structure−Activity Relationship Studies

Zhichao Zhang,*[,†] Guiye Wu,[†,∥] Feibo Xie,[†,‡,∥] Ting Song,[§] and Xilong Chang[§]

[†]*School of Chemistry, Dalian University of Technology, Dalian 116012, People's Republic of China,* [‡]*State Key Laboratory of Elemento-Organic Chemistry, Nankai University, Tianjin 300071, People's Republic of China, and* [§]*School of Life Science and Technology, Dalian University of Technology, Dalian 116024, People's Republic of China.* [∥] *These authors contributed equally to this work.*

Received September 10, 2010

We recently described the discovery of a dual inhibitor of Bcl-2 and Mcl-1, 3-thiomorpholin-8-oxo-8*H*-acenaphtho[1,2-*b*]pyrrole-9-carbonitrile (**3**, S1). Here we report a structure-guided design in combination with structure−activity relationship studies to exploit the difference in the p2 binding pocket of Bcl-2 and Mcl-1, from which a novel dual inhibitor 3-(4-aminophenylthio)-8-oxo-8*H*-acenaphtho[1,2-*b*]pyrrole-9-carbonitrile (**6h**) was obtained, which showed significant enhanced IC_{50} value against Mcl-1 (5 nM), greater Mcl-1/Bak disruption potential, and accordingly a 10-fold increased cytotoxicity over **3**.

Introduction

Members of the Bcl-2[a] family of proteins are key regulators of apoptosis. This family possesses antiapoptotic and proapoptotic members.[1] A balance between antiapoptotic and proapoptotic members dictates a cell's fate and is mediated by the BH3 domain of the BH3-only proteins inserting into a hydrophobic groove on the surface of prosurvival proteins including Bcl-2, Bcl-x_L, and Mcl-1.[2,3] Therefore, small molecules that mimic BH3-only proteins and can occupy the BH3 groove may neutralize Bcl-2-like proteins, liberate proapoptotic Bax/Bak, or activate them directly. These artificial BH3 mimetics are thought to disable the antiapoptotic function and thus induce tumor cells apoptosis.[4]

Although more than dozens of BH3 mimetics have been reported, none are in clinical use.[4] Specificity and pan-Bcl-2 inhibition are the most challenging issues.[5] The most authentic BH3 mimetic **4** (ABT737), for example, is not a pan-Bcl-2 inhibitor. The inability to target a more divergent prosurvival relative, the Mcl-1 protein, elicits the resistance of many cancer cell lines to **4**.[6,7]

Recent studies argue that Mcl-1 has a critical and distinct role in the regulation of apoptosis.[8] It has been well established that a "pan-Bcl-2 inhibitor" should be a compound that may not bind to all of the Bcl-2-like proteins but that can bind to at least Bcl-2 and Mcl-1 to disarm the prosurvival capacities of these key targets.[4] Such "dirty drugs" may prove successful in clinical development. As such, the potential for novel compounds that hit Bcl-2 and Mcl-1 may rest for the time being in the organic chemistry lab.

We have previously reported the existence of a small-molecule Bcl-2 inhibitor, 3-thiomorpholin-8-oxo-8*H*-acenaphtho[1,2-*b*]pyrrole-9-carbonitrile (**3**, S1).[9] The in vivo apoptosis induction by **3** places it on the list of 19 preclinical Bcl-2 inhibitor antitumor drugs.[10] Further studies have described the characteristic properties of **3** as an authentic BH3 mimetic and a pan-Bcl-2 inhibitor that targets Bcl-2 and Mcl-1.[11,12] The single agent antitumor activity against primary acute lymphoblastic leukemia (ALL) cells regardless of Mcl-1 levels and in a xenograft model has notable implications for **3** and its derivatives becoming novel antitumor drugs. Here, we designed a series of analogues based on solution-based binding studies of **3** with expressed Mcl-1 protein and on 3D docking studies of **3** with human Bcl-2 and Mcl-1.

Results and Discussion

Rationale. Our previous studies identified **3** (Scheme 1) as the first authentic BH3 mimetic and a dual, nanomolar inhibitor of Bcl-2 and Mcl-1 (K_i = 310 and 58 nM, respectively).[11] Consistent with the stronger affinity of **3** for Mcl-1 over Bcl-2, the Mcl-1/Bak complex was more readily disrupted by **3** in cell-based and in vivo experiments. This observation prompted us to explore the dual binding profile of **3**. First, we considered the previous structural analysis of the Bim BH3 peptide in complex with the Bcl-x_L, Bcl-2, and Mcl-1 proteins. This analysis showed that four conserved hydrophobic residues (h1−h4) on one face of a Bim helix are inserted into four hydrophobic pockets (p1−p4) within the grooves of all three proteins (Figure 1a and Figure 1b).[13−15] Another crucial residue aspartate D67, which was able to form a salt bridge with arginine in prosurvival proteins, was also found to be important.[13] Second, we analyzed the predicted structures of **3** in complex with human Mcl-1 and

*To whom correspondence should be addressed. Phone: 86-411-39893872. Fax: 86-411-83673488. E-mail: zczhang@dlut.edu.cn.

[a] Abbreviations: Bcl-2, B-cell lymphoma 2; Mcl-1, myeloid cell leukemia sequence 1; Bim, Bcl-2 interacting mediator of cell death; Bid, BH3 interacting domain death agonist; Bcl-x_L, B-cell lymphoma x long; Bax, Bcl-2-associated X protein; Bak, Bcl-2 homologous antagonist/killer; Bad, Bcl-2 antagonist of cell death; SAR, structure−activity relationship; FPA, fluorescence polarization assay; K_i, inhibition constant; K_d, dissociation constant; HPLC, high-performance liquid chromatography; ELISA, enzyme-linked immunosorbent assay; ADT, AutoDockTools.

Published on Web 01/14/2011

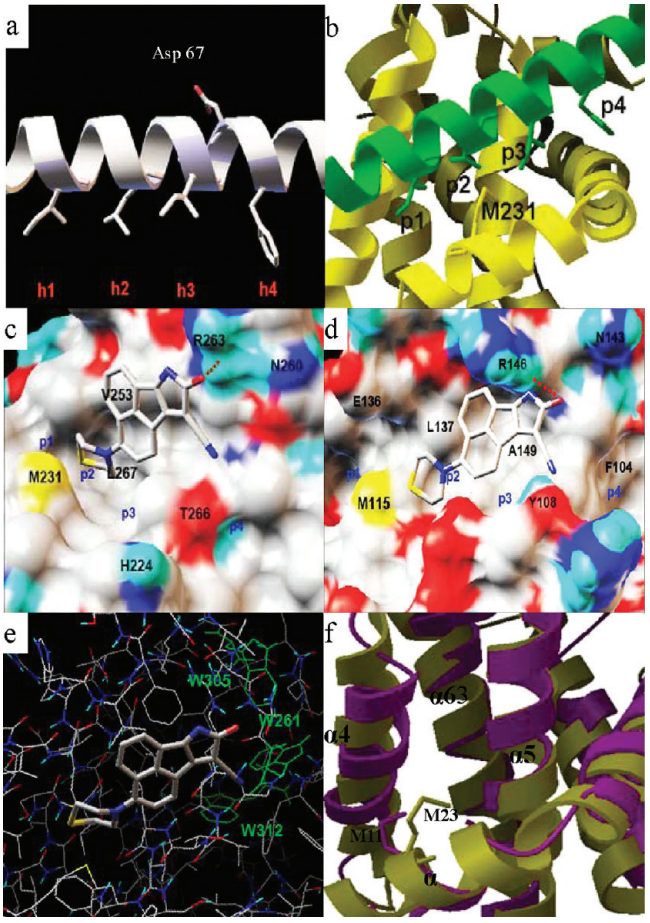

Figure 1. (a) The relative locations of the four crucial hydrophobic residues of Bim are indicated h1−h4. The side chain for D67 of the Bim peptide is also displayed. (b) Aligned four pockets of Mcl-1 and four crucial hydrophobic residues of the Bim BH3 peptide. The BH3 peptide is shown in a green helix. M231 is located in the p2 pocket. (c) Predicted binding model of **3** in complex with Mcl-1 and (d) Bcl-2. Mcl-1 and Bcl-2 are shown in a surface representation, and the carbon, oxygen, nitrogen, and sulfur atoms are shown in gray, red, blue, and yellow, respectively. These atoms are labeled in **3** using the same color as for the proteins. Hydrogen bonds are depicted in dotted lines in red. (e) Predicted binding region involved three tryptophan residues of Mcl-1. (f) Overlay of the structures of Mcl-1 (yellow) and Bcl-2 (pink). The M231 is more exposed than M115.

Scheme 1. Structures of **3**, **5a**−**g**, **6a**−**i**, and **9h**,**i**

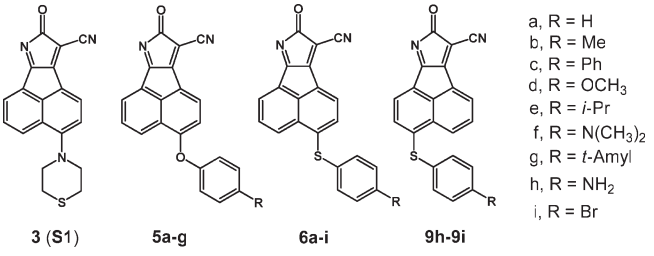

Bcl-2 with the help of computational modeling studies using AutoDock 4.0 (Figure 1c and Figure 1d, respectively). These studies revealed that **3** lies along a hydrophobic binding pocket of Mcl-1 in an orientation similar to that of Bcl-2. **3** occupies the p2 and p3 pockets of Bcl-2 and Mcl-1. The carbonyl group of **3** binds close to R146 of Bcl-2 and R263 of Mcl-1. Accordingly, a hydrogen bonding network could be formed between the carbonyl group of **3** and arginine. The similar positioning of R146 of Bcl-2 and R263 of Mcl-1 in their three-dimensional structure allows **3** to bind in similar orientations within their BH3 binding grooves. Subsequent solution-based binding studies provided further confirmation of the predicted docking results. (See Supporting Information).

Notably, the p2 pocket of Mcl-1 is significantly different from its counterpart on Bcl-2. Phage display studies combined with saturation mutagenesis have revealed that the p2 pocket of Mcl-1 is more constricted than that of Bcl-x_L.[14] The p2 pocket of Bcl-2 is even wider than that of Bcl-x_L.[17] So the p2 pocket of Mcl-1 is not as tolerant as that of Bcl-2. Consistently, our computational modeling studies illustrated that the solvent-exposed M231 of Mcl-1 decreases the width of the p2 pocket much more than the p2 pocket of Bcl-2 (Figure 1b and Figure 1f), consistent with the previous finding that M231 prevents engagement of the Bad BH3 peptide by spatial confliction.[18] Additionally, the p2 pocket is the deepest of the four pockets of Mcl-1.[14] As such, the occupation of p2 may help dictate which molecules hit Mcl-1. The nanomolar affinity of **3** for Mcl-1 may be attributed to the binding of thiomorpholine into the p2 pocket.

To gain insight into the dual binding of **3** to Bcl-2 and Mcl-1, to explore the functional group, and to investigate the possibility of utilizing the structural scaffold found in **3** for a future pan-Bcl-2 inhibitor, a series of derivatives were synthesized and evaluated. Because the carbonyl substitution was thought to contribute largely to the binding affinity of the two proteins, we selected thiomorpholine as the starting point to probe the interaction surface of **3** and proteins, especially for the investigation of how the p2 pocket is accommodated on Mcl-1. We hypothesized that a substituent with the proper steric bulk that mimics the corresponding residues on the BH3 peptide may access the deep p2 pocket and enhance the affinity to Mcl-1 without adversely affecting the affinity for Bcl-2, as the p2 pocket of Bcl-2 is wider. We therefore began by replacing thiomorpholine with groups of various sizes.

Structure−Activity Relationships. First, we substituted the thiomorpholine using oxygen or sulfur atoms as a linker, which renders flexibility to compounds, allowing them to engage well into the p2 pocket. Specifically, we examined phenyl, 4-methylphenyl, 4-biphenyl, and 4-methoxyphenyl groups, yielding analogues 3-phenoxy-8-oxo-8*H*-acenaphtho-[1,2-*b*]pyrrole-9-carbonitrile (**5a**), 3-(*p*-tolyloxy)-8-oxo-8*H*-acenaphtho[1,2-*b*]pyrrole-9-carbonitrile (**5b**), 3-(biphenyl-4-yloxy)-8-oxo-8*H*-acenaphtho[1,2-*b*]pyrrole-9-carbonitrile (**5c**), 3-(4-methoxyphenoxy)-8-oxo-8*H*-acenaphtho[1,2-*b*] pyrrole-9-carbonitrile (**5d**) and 3-phenylthio-8-oxo-8*H*-acenaphtho[1,2-*b*]pyrrole-9-carbonitrile (**6a**), 3-(4-methylphenylthio)-8-oxo-8*H*-acenaphtho[1,2-*b*]pyrrole-9-carbonitrile (**6b**), 3-(4-biphenylthio)-8-oxo-8*H*-acenaphtho[1,2-*b*]pyrrole-9-carbonitrile (**6c**), 3-(4-methoxyphenylthio)-8-oxo-8*H*-acenaphtho[1,2-*b*]pyrrole-9-carbonitrile (**6d**), respectively (Scheme 1). The binding affinities (K_i) of the compounds were evaluated using fluorescence polarization assays (FPAs) that measure their abilities to competitively displace a Bid-derived peptide from Mcl-1, as described in the Supporting Information. The competitive binding curves of these compounds to Mcl-1 are outlined in Figure 2a and Figure 2b. The K_i of **3** toward Mcl-1 was 62 nM in this measurement, which is a little different from that of our previous publication (58 nM) because we added Triton X-100 this time as a detergent to prevent the possible aggregation of hydrophobic compounds. A progressive increase in steric bulk of the substituent (**a** < **b** < **c** < **d**) resulted in a corresponding increase in Mcl-1 affinity. While no

binding to Mcl-1 was found for **5a** and **6a** (K_i > 100 μM), the K_i achieved 258 and 151 nM for **5d** and **6d**, respectively.

The significantly improved binding of **5d** and **6d** encouraged us to further prolong the substituent at the para position of the phenyl group. Isopropyl-3-(4-isopropylphenoxy)-8-oxo-8*H*-acenaphtho[1,2-*b*]pyrrole-9-carbonitrile (**5e**), 3-(4-isopropylthiophenol)-8-oxo-8*H*-acenaphtho[1,2-*b*]pyrrole-9-carbonitrile (**6e**), *N*,*N*-dimethylamino-3-(4-*N*,*N*-dimethylaminophenoxy)-8-oxo-8*H*-acenaphtho[1,2-*b*]pyrrole-9-carbonitrile (**5f**), 3-(4-*N*,*N*-dimethylaminophenylthio)-8-oxo-8*H*-acenaphtho[1,2-*b*]pyrrole-9-carbonitrile (**6f**)), and larger *tert*-amyl analogues 3-(4-*tert*-amylphenoxy)-8-oxo-8*H*-acenaphtho[1,2-*b*]pyrrole-9-carbonitrile (**5g**) and 3-(4-*tert*-amylthiophenol)-8-oxo-8*H*-acenaphtho[1,2-*b*]pyrrole-9-carbonitrile (**6g**) were explored (Scheme 1). More importantly, isopropyl, *N*,*N*-dimethylamino, and *tert*-amyl motifs may partly mimic the isobutyl group of L62 in the Bim BH3 peptide based on crystallographic studies.[19] As expected, the K_i of **5e** (99 nM) was nearly half that of **5d** (258 nM). Comparably, **5f** showed a K_i of 122 nM. Significant improvements were also found for **6e** (82 nM) and **6f** (91 nM), whose affinities were about 2-fold higher than **6d** (151 nM). **5g** (967 nM) and **6g** (961 nM), however, were 10 times less potent than **5e** and **6e** (Figure 2a and Figure 2b). As shown in Figure 3a and Figure 3b, the docking studies further demonstrated that the isopropyl and *N*,*N*-dimethylamino groups indeed mimic the interactions of L62 in Bim with Mcl-1. **5g** and **6g**, however, cannot accommodate well inside the p2 pocket because of steric hindrance.

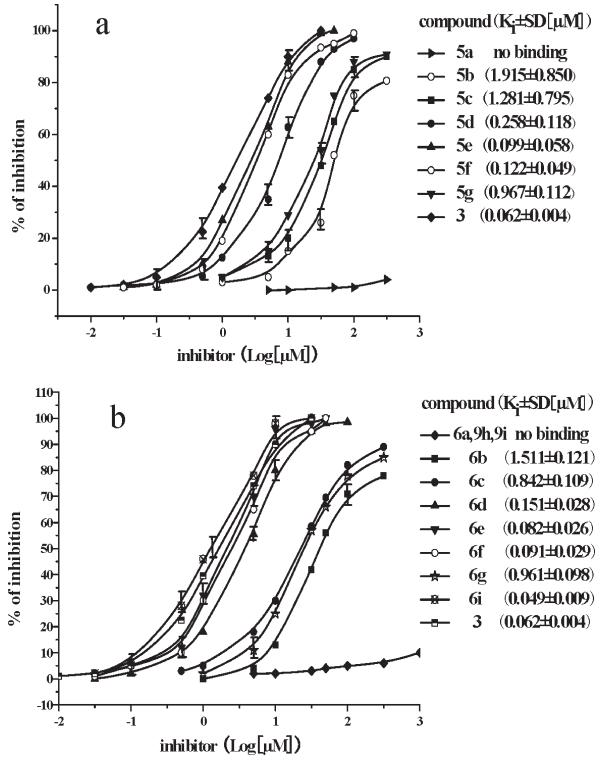

Figure 2. Binding affinities of (a) **5a**−**g** to Mcl-l and (b) **6a**−**i**, **9h**, **9i** to Mcl-l by FPAs.

The SAR studies further confirmed that the isopropyl motif, *N*,*N*-dimethylamino group, and thiomorpholine group of their parent (**3**) are located in the p2 pocket. Furthermore, we found that these motifs are close to the carbonyl of L267 (Figure 3a). Amino groups can form hydrogen bonds with carbonyl groups. Therefore, although L267 is a hydrophobic residue, a hydrogen bond may still be available as previously reported.[19] To generate an additional hydrogen bond, we replaced the *N*,*N*-dimethylamino group by an amino group. Because the **6** series of compounds had stronger binding affinities than the **5** series and a more synthetically tractable core, we designed **6h** (Scheme 1). As expected, a hydrogen bond is formed between the amino group of **6h** and the carbonyl of L267 (Figure 3c).

Unfortunately, FPA can be influenced by the autofluorescence of **6h**. Therefore, we applied an enzyme-linked immunosorbent assay (ELISA) for Mcl-1 (Supporting Information).We detected a significant enhanced IC_{50} for **6h** (5 nM), compared with that of **3** (35 nM) (Table 1). Consistent with the much less potential affinity measured by FPA, **6g** exhibited 585 nM IC_{50} that is also much weaker than **3** by ELISA.

We next compare the targeting ability of **3** and **6h** toward Mcl-1 inside living cells by using coimmunoprecipitation (co-IP). **3** has been verified in our previous publication to induce apoptosis by neutralizing the intrinsic overexpressed Bcl-2 and Mcl-1 in the human liver cancer cell line (SMMC-7721), human breast adenocarcinoma cell line (MCF-7), and SMMC-7721 cells transfected with Mcl-1 expression plasmid (SMMC-7721/Mcl-1).[11] Here, we tested the disruption of cellular Mcl-1/Bak by **3**, **6g**, and **6h** in parallel with the three cell lines (Figure 4). **6a** was used as a negative control.

Table 1. Competitive Binding of **3**, **6g**, and **6h** to Mcl-1 and Bcl-2 Protein As Determined Using an ELISA Assay (IC_{50}, μM)[a]

protein	3	6g	6h
Mcl-1	0.035 ± 0.014	0.585 ± 0.095	0.005 ± 0.001
Bcl-2	0.285 ± 0.065	0.342 ± 0.083	0.302 ± 0.048

[a] Values are the mean ± standard deviation of three independent experiments.

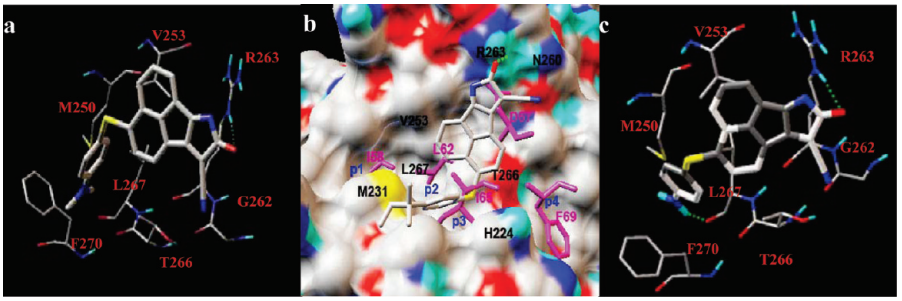

Figure 3. Predicted binding models of Mcl-1 in complex with (a) **6f**, (b) **6g**, and (c) **6h**. The carbon, oxygen, nitrogen, and sulfur atoms of Mcl-1 and indicated compounds are shown in gray, red, blue, and yellow, respectively. Key residues in the Bim BH3 peptide are shown and labeled in pink. Hydrogen bonds are depicted as green dashed lines.

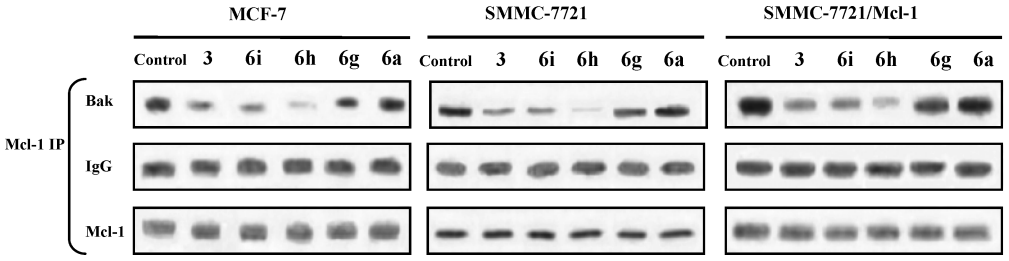

Figure 4. Disruption of Mcl-1/Bak interaction by **3**, **6i**, **6h**, **6g**, and **6a**, respectively. Co-IP method was used. MCF-7, SMMC-7721 and SMMC-7721/Mcl-1 cells were treated with 10 μM of each compound for 3 h. Lysates equivalent to 100 μg of protein were prepared. Bak was immunoprecipitated, and the immunoprecipitates were subjected to western blot analysis using anti-Mcl-1 antibody. Cells treated with vehicle (DMSO) were measured as control. Results are expressed as mean ± SEM of three independent experiments.

Table 2. Cytotoxicity Evaluation of **3**, **6g**, **6h**, **6i**, and **6a** against Tumor Cell Lines (IC_{50}, μM)[a]

tumor line	3	6g	6h	6i	6a
MCF-7	0.09 ± 0.01	21.33 ± 1.14	0.012 ± 0.003	0.09 ± 0.03	> 50
MMC-7721	0.17 ± 0.001	11.90 ± 0.97	0.018 ± 0.010	0.19 ± 0.01	> 50
SMMC-7721/Mcl-1	0.19 ± 0.001	25.55 ± 1.21	0.016 ± 0.009	0.18 ± 0.05	> 50
HEK 293	> 100	> 50	> 50	> 50	> 50

[a] The IC_{50} value was obtained through MTT assay (Supporting Information).Values are the mean ± standard deviation of three independent experiments.

As expected, **6a** did not show any disruption while **6h** exhibited much greater disruption potential than **3** at the same concentration and for the same exposure time. The disruption ability of **6g** is much less potent than **6h**. Of note, the high level of Mcl-1 in SMMC-7721/Mcl-1 cells did not prevent the disruption of **6h**, just like its parent **3**. Consistently, the IC_{50} of these compounds in the three cell lines decreased in the order **6a** > **6g** > **3** > **6h** (Table 2). Meanwhile, the compounds activated caspase 3 in SMMC-7721 cells in the same order as their IC_{50} and the levels of Mcl-1/Bak disruption (Figure S4). These data demonstrated that, like **3**, **6h** can exhibit mechanism-based apoptosis induction in multiple cancer cells. The cytotoxicity of **6a**, **6g**, **6h**, and **3** was also tested against normal cell line HEK 293 (human embryonic kidney cell line 293). Consistent with their mechanism-based antitumor activities, **3** and **6h** exhibited almost no cytotoxicity on normal cells. Most notably, **6h** exhibited approximately 10-fold enhanced cytotoxicity against cancer cells compared to **3**. We were interested in whether the surprisingly increased cytotoxicity is indeed due to the additional hydrogen bond. We therefore designed 3-(4-bromophenylthio)-8-oxo-8*H*-acenaphtho[1,2-*b*]pyrrole-9-carbonitrile (**6i**), in which a bromine group replaced the amino group. On one hand, the bromine atom and amino group are bioisosteric.[20] On the other hand, it has been revealed that halogen bonds (X···O interactions) are comparable in magnitude to classical hydrogen bonding.[21] The strength of the interactions attenuates in the order H ∼ I > Br > Cl.[21] We were interested in comparing the inhibition of **6h** and **6i**.

By FPA, **6i** exhibited a K_i (49 nM) comparable with that of **3** (Figure 2b), reflecting comparable disruption and caspase 3 activation with **3** in the above-mentioned cancer cell lines (Figure 4 and Figure S4). Although **6i** can also exhibit mechanism-based apoptosis induction in multiple cancer cells, its antagonistic ability against Mcl-1 is less potent than **6h**, returning to the level of **3**. It is reasonable to suggest that this occurs because the halogen bond formed by the bromine group is weaker than the hydrogen bond formed by the amino group, resulting in a decrease of antagonistic ability.

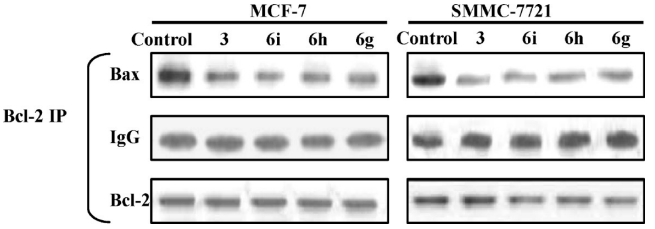

Figure 5. Disruption of Bcl-2/Bax complex in MCF-7 and SMMC-7721 cells by **3**, **6i**, **6h**, and **6g**, respectively. Co-IP method was used. Cells treated with 10 μM of each compound for 3 h. Specific antibodies were used. Cells treated with vehicle (DMSO) were measured as control.

Accordingly, we verified that the enhanced antagonism of **6h** against Mcl-1 was due to hydrogen bonding.

So far, two novel nanomolar Mcl-1 inhibitors, **6h** and **6i**, have been discovered using S1-based design assisted by computational modeling and SAR. We tested whether they maintained the binding ability of **3** to Bcl-2 using FPA. We determined that the K_i of **6i** was 382 nM (Figure S1), similar to that of **3** (319 nM). The antagonism of **6h** against Bcl-2 was determined using co-IP and compared with **3** and **6i**. The results showed that the three molecules disrupted Bcl-2/Bax similarly in MCF-7 and SMMC-7721 cancer cell lines (Figure 5).

Interestingly, the antagonism of **6g** whose inhibition of Mcl-1 is less potent than **3** against Bcl-2 was also tested using FPA and co-IP. The result showed a similar K_i (355 nM) to that of **3** (319 nM, Figure S1). It also translated into a similar disruption of Bcl-2/Bax with **3** (Figure 5). Compared to **6i**, the larger substituent *tert*-amyl of **6g** was still tolerated by Bcl-2 but was excluded by Mcl-1. To some extent, it confirmed the docking result and the previous finding that the binding pocket of Bcl-2 is wider and more accommodating than that of Mcl-1, especially the p2 pocket. As such, we suspected that an appropriate hindrance may provide a balanced dual inhibition of Bcl-2 and Mcl-1. In addition, the antagonism of **6g** against Bcl-2 may provide an explanation for its relatively weaker caspase 3 activation (Figure S4) and micromolar cytotoxicity (Table 2). Additionally, the comparable antagonism of **3**, **6g**, and **6h** against Bcl-2 was verified by ELISA (Table 1).

Next, we further demonstrate that the carbonyl substitution of **3** plays a key role in binding to Bcl-2 and Mcl-1 due to the hydrogen bond formed between this group and arginine (Supporting Information).

Conclusions

Utilizing our previous finding, **3**, as a template and using structure-guided design, we examined a series of potent dual inhibitors of Bcl-2 and Mcl-1. Compound **6i** exhibited

a nanomolar K_i with Mcl-1 and a nanomolar IC_{50} against SMMC7721 cells, similar to the initial compound **3**. Excitingly, **6h** is much more effective, with a 10-fold lower IC_{50} than **3**. It not only enhanced the affinity to Mcl-1 but also maintained the affinity to Bcl-2. The improved affinity of **6h** in vitro also translated to enhanced intracellular disruption of the heterodimerization of Mcl-1/Bak, which induced more caspase 3 activation in a dose-dependent manner. These studies strongly suggested that **6h** exhibited antitumor properties through inhibition of Bcl-2/Mcl-1 and was much more efficient than **3**. Extensive studies are in progress to ascertain its therapeutic potential.

In addition, the binding orientation and positioning of **3** and its derivatives were examined using solution-based binding studies, docking studies, and SAR studies. The carbonyl substitution of **3** binds near R146 of Bcl-2 and R263 of Mcl-1 through hydrogen bonds, whereas the 3-position substituent extends into the p2 pocket. More importantly, our working hypothesis for accessing a deep p2 pocket of Mcl-1 was confirmed throughout this study. Enhanced affinity could be achieved using a proper 3-position group, mimicking the Bim BH3 peptide, together with the creation of additional hydrogen bonds. The geometry and bulk of an isopropyl group are appropriate to hit the p2 pocket of Bcl-2 and Mcl-1. A *tert*-amyl group, however, is more suitable for Bcl-2 than Mcl-1. This illustrated the difference between the p2 pocket of Bcl-2 and Mcl-1.

Taken together, our data indicated that **3** and its derivates represent attractive templates for a future "dirty drug" that functions to kill tumor cells by a canonical machine-based model of action.

Experimental Section

The synthesis of **6h** and **6i** is shown in Supporting Information Scheme 2. **6h**. Yield: 0.05 g, 33%. ^{1}H NMR (400 MHz, $CDCl_3$): δ 8.86 (d, J = 8.0 Hz, 1H), 8.82 (d, J = 8.0 Hz, 1H), 8.02 (d, J = 8.4 Hz, 1H), 7.95 (t, J = 8.0 Hz, 1H), 7.48 (d, J = 8.48 Hz, 2H), 7.05 (d, J = 8.4 Hz, 2H), 6.83 (d, J = 8.4 Hz, 1H), 3.42(br, 2H). TOF MS (EI^+): $C_{21}H_{11}N_3OS$, calcd for 353.0623, found 353.0625. HPLC system 2: purity = 98.43%, t_R = 20.99 min.

6i. Yield: 0.07 g, 35%. ^{1}H NMR (400 MHz, $CDCl_3$): δ 8.86 (d, J = 8.4 Hz, 1H), 8.81 (d, J = 8.4 Hz, 1H), 8.01 (d, J = 8.0 Hz, 1H), 7.96 (t, J = 8.0 Hz, 1H), 7.56 (d, J = 8.8 Hz, 2H), 7.09 (d, J = 8.8 Hz, 2H), 7.00 (d, J = 8.0 Hz, 1H). TOF MS (EI^+): $C_{21}H_9N_2OSBr$, calcd for 415.9619, found 415.9628. HPLC system 2: purity = 98.5%, t_R = 15.88 min.

Acknowledgment. This work was supported by the National Natural Science Foundation of China (Grant 30772622) and partly supported by the Fundamental Research Funds for the Central Universities.

Supporting Information Available: Full experimental details, ^{1}H NMR and HRMS spectra, and characterization data. This material is available free of charge via the Internet at http://pubs.acs.org.

References

(1) Willis, S. N.; Adams, J. M. Life in the balance: how BH3-only proteins induce apoptosis. *Curr. Opin. Cell. Biol.* **2005**, *17*, 617–625.
(2) Cory, S.; Huang, D. C.; Adams, J. M. The Bcl-2 family: roles in cell survival and oncogenesis. *Oncogene* **2003**, *22*, 8590–8607.
(3) Fleischer, A.; Rebollo, A.; Atkkib, V. BH3-only proteins: the lords of death. *Arch. Immunol. Ther. Exp.* **2003**, *51*, 9–17.
(4) Azmi, A. S.; Mohammad, R. M. Non-peptidic small molecule inhibitors against Bcl-2 for cancer therapy. *J. Cell. Physiol.* **2009**, *218*, 13–21.
(5) Delft, M. F. V.; Wei, A. H.; Mason, K. D.; Vandenberg, C. J.; Chen, L.; Czabotar, P. E.; Willis, S. N.; Scott.C. L.; Day, C. L.; Cory, S.; Adams, J. M.; Roberts, A. W.; Huang, D. C. S. The BH3 mimetic ABT-737 targets selective Bcl-2 proteins and efficiently induces apoptosis via Bak/Bax if Mcl-1 is neutralized. *Cancer Cell* **2006**, *10*, 389–399.
(6) Konopleva, M.; Contractor, R.; Tsao, T.; Samudio, I.; Ruvolo, P. P.; Kitada, S.; Deng, X.; Zhai, D.; Shi, Y. X.; Sneed, T.; Verhaegen, M.; Soengas, M.; Ruvolo, V. R.; McQueen, T.; Schober, W. D.; Watt, J. C.; Jiffar, T.; Ling, X.; Marini, F. C.; Harris, D.; Dietrich, M.; Estrov, Z.; McCubrey, J.; May, W. S.; Reed, J. C.; Andreeff, M. Mechanisms of apoptosis sensitivity and resistance to the BH3 mimetic ABT-737 in acute myeloid leukemia. *Cancer Cell* **2006**, *10*, 375–388.
(7) Kang, M. H.; Wan, Z. S.; Kang, Y. H.; Sposto, R.; Reynolds, C. P. Mechanism of synergy of *N*-(4-hydroxyphenyl) retinamide and ABT-737 in acute lymphoblastic leukemia cell lines: Mcl-1 inactivation. *J. Natl. Cancer. Inst.* **2008**, *8*, 580–595.
(8) Warr, M. R.; Shore, G. C. Unique biology of Mcl-1: therapeutic opportunities in cancer. *Curr. Mol. Med.* **2008**, *8*, 138–147.
(9) Zhang, Z.; Jin, L.; Qian, X.; Wei, M.; Wang, Y.; Wang, J.; Yang, Y.; Xu, Q.; Xu, Y.; Liu, F. Novel Bcl-2 inhibitors: discovery and mechanism study of small organic apoptosis-inducing agents. *ChemBioChem* **2007**, *8*, 113–121.
(10) Fischer, U.; Janssen, K.; Osthoff, K. S. Cutting-edge apoptosis-based therapeutics. *BioDrugs* **2007**, *21*, 273–297.
(11) Zhang, Z.; Song, T.; Zhang, T.; Wu, G.; Gao, J.; An, L.; Du, G. A novel BH3 mimetic S1 potently induces Bax/Bak-dependent apoptosis by targeting both Bcl-2 and Mcl-1. *Int. J. Cancer* [Online early access]. DOI: 1002/ijc.25484. Published online: May 25, 2010.
(12) Qian, X.; Zhang, Z.; Xiao, Y.; Liu, F.; Lu, Z. Acenaphtho Heterocycle Compounds and the Uses in the Induce Apoptosis and Antitumor. CN Patent Appl. 200410050449.5; Sep, 15, 2004.
(13) Lee, E. F.; Czabotar, P. E.; Smith, B. J.; Deshayes, K.; Zobel, K.; Colman, P. M.; Fairlie, W. D. Crystal structure of ABT-737 complexed with Bcl-xL: implications for selectivity of antagonists of the Bcl-2 family. *Cell Death Differ.* **2007**, *14*, 1711–1719.
(14) Czabotar, P. E.; Lee, E. F.; van Delft, M. F.; Day, C. L.; Smith, B. J.; Huang, D. C. S.; Douglas Fairlie, W.; Hinds, M. G.; Colman, P. M. Structural insights into the degradation of Mcl-1 induced by BH3 domains. *Proc. Natl. Acad. Sci. U.S.A.* **2007**, *104*, 6217–6222.
(15) Wang, G.; Nikolovska-Coleska, Z.; Yang, C.; Wang, R.; Tang, G.; Guo, J.; Shangary, S.; Qiu, S.; Gao, W.; Yang, D.; Meagher, J.; Stuckey, J.; Krajewski, K.; Jiang, S.; Roller, P. P.; Abaan, H. O.; Tomita, Y.; Wang, S. Structure-based design of potent small-molecule inhibitors of anti-apoptotic Bcl-2 proteins. *J. Med. Chem.* **2006**, *49*, 6139–6142.
(16) Etxebarria, A.; Landeta, O.; Antonsson, B.; Basañez, G. Regulation of antiapoptotic MCL-1 function by gossypol: mechanistic insights from in vitro reconstituted systems. *Biochem. Pharmacol.* **2008**, *76*, 1563–1576.
(17) Bruncko, M.; Oost, T. K.; Belli, B. A.; Ding, H.; Joseph, M. K.; Kunzer, A.; Martineau, D.; McClellan, W. J.; Mitten, M.; Ng, S.-C. Nimmer, P. M.; Oltersdorf, T.; Park, C.-M.; Petros, A. M.; Shoemaker, A. R.; Song, X.; Wang, X.; Wendt, M. D.; Zhang, H.; Fesik, S. W.; Rosenberg, S. H.; Elmore, S. W. Studies leading to potent, dual inhibitors of Bcl-2 and Bcl-xL. *J. Med. Chem.* **2007**, *50*, 641–662.
(18) Liu, Q.; Moldoveanu, T.; Sprules, T.; Matta-Camacho, E.; Mansur-Azzam, N.; Gehring, K. Apoptotic regulation By Mcl-1 through heterodimerization. *J. Biol. Chem.* **2010**, *285*, 19615–19624.
(19) Tang, G.; Ding, K.; Nikolovska-Coleska, Z.; Yang, C.-Y.; Qiu, S.; Shangary, S.; Wang, R.; Guo, J.; Gao, W.; Meagher, J.; Stuckey, J.; Krajewski, K.; Jiang, S.; Roller, P. P.; Wang, S. Structure-based design of flavonoid compounds as a new class of small-molecule inhibitors of the anti-apoptotic Bcl-2 proteins. *J. Med. Chem.* **2007**, *50*, 3163–3166.
(20) Lima, L. M.; Barreiro, E. J. Bioisosterism: a useful strategy for molecular modification and drug design. *Curr. Med. Chem.* **2005**, *12*, 23–49.
(21) Lu, Y.; Shi, T.; Wang, Y.; Yang, H.; Yan, X.; Luo, X.; Jiang, H.; Zhu, W. Halogen bondings—a novel interaction for rational drug design? *J. Med. Chem.* **2009**, *52*, 2854–2862.